Prediction of Surface settlement in Shield Tunneling Construction Process using PCA-PSO-RVM Machine Learning

Yan Zhang[1], Zicheng Wang[2], Hewei Kuang[3], Feng Fu[4], CEng, F.ASCE,Aiping Yu[5]

Abstract:

Surface settlement is one of the key engineering issues during shield construction process. In order to accurately predict surface settlement, this paper proposes a new machine learning method based on Relevance Vector Machine (RVM), Principal Component Analysis (PCA) and Particle Swarm Optimization (PSO). Taking Beijing Metro Line 6 as an case study, the PCA-PSO-RVM model is used to make the prediction and compared with the prediction results of the RVM model using the same samples. In order to evaluate the reliability of the model, three evaluation indexes including mean relative error (MRE), root mean square error (RMSE) and Theil inequality coefficient (TIC) were calculated, and sensitivity analysis was carried out on them. The results show that the minimum relative error between PCA-PSO-RVM and the actual value is only 0.06%. The calculated MRE, RMSE and TIC are 0.17%, 0.0714 and 0.027% respectively, which shows that PCA-PSO-RVM model has higher prediction accuracy, smaller deviations and higher reliability compared with other three models. Through sensitivity analysis, it is found that the weighted average internal friction angle (φ) has the most significant impact on the surface settlement, which should be focused on in relevant research.

Keywords: shield tunneling; surface settlement; principal component analysis; particle swarm optimization; correlation vector machine; prediction model

1. Yan Zhang Professor， College of Civil and Architectural Engineering, Guilin University of Technology, Guilin 541004. zhangyan@glut.edu.cn;
2. Zicheng Wang, Master Degree Candidate，College of Civil and Architectural Engineering, Guilin University of Technology, Guilin 541004. 1271229848@qq.com;

3. Hewei Kuang Master Degree Candidate， College of Civil and Architectural Engineering, Guilin University of Technology, Guilin 541004. chenxuandong@glut.edu.cn;
4. Feng Fu, Associate Professor, Department of Civil Engineering, School of Mathematics, Computer Science & Engineering, City, University of London, Northampton Square, London, EC1V 0HB,U.K.College of Civil and Architectural Engineering, Adjunct Professor Guilin University of Technology, Guilin 541004. (Corresponding author), feng.fu.1@city.ac.uk
5 Aiping Yu [1], Professor， College of Civil and Architectural Engineering, Guilin University of Technology, Guilin 541004. apyu@glut.edu.cn；

1 Introduction

With the development of urbanization, the urban traffic congestion increases day by day, and the development and utilization of underground space has become high demand in urban traffic development (Azhdar and Nazemi, 2020; Du and Zheng, 2020). The shield tunneling method is widely used in subway construction due to its advantages of high precision, good safety and self-control feature. During the tunneling process, the stratum suffers different degrees of displacement and settlement, which may cause serious tunnel damage, ground subsidence, surface pipeline damage, and surrounding buildings damage (Zhou *et al.*, 2019; Liu *et al.*, 2020). Therefore, the prediction of surface settlement during shield construction has become an important research topic. The effective assessment of surface settlement provides guidance for subway construction and provides basis for protection measures for surrounding buildings (Singh *et al.*, 2018; Zhang *et al.*, 2021).

The surface settlement of shield tunneling is affected by many factors. Each factor interacts and influences each other. It is difficult to accurately determine the surface settlement. Many scholars have paid attention to the complexity of this problem and have carried out a series of related Research (Kasper and Meschke, 2006; Chen *et al.*, 2019). The research methods of surface settlement of shield tunneling construction mainly include empirical method (Sharghi *et al.*, 2017), theoretical analysis (Verruijt and Booker, 1998; Chou and Bobet, 2002) and neural network prediction using machine learning (Wang *et al.*, 2013; Ocak and Seker, 2013). Peck (1969) proposed in 1969 that the morphological distribution of the settlement tank in tunnel follows normal distribution. Based on the theory of ground loss (Li *et al*., 2021), a formula for estimating the surface settlement of a circular tunnel is proposed, which is currently the most widely used. On the basis of this formula, many theoretical studies and settlement formula calculations have been developed and widely used. However, the geological conditions during shield construction are complicated and various parameters during the excavation process will affect the surface settlement, and these parameters are uncertain, and it is difficult to use a simple formula to establish the relationship between surface settlement and influencing factors.

In recent years, with the rapid development of computer technologies, machine learning methods based on artificial intelligence stand out and are widely used in the study of nonlinear problems in various engineering fields. Salimi *et al*., (2016) used two different artificial neural network models to predict the working efficiency of TBM tunnel construction in hard rock based on actual engineering projects. The results show that artificial neural network has good adaptability and accuracy. On this basis, the use of optimization algorithms to improve the accuracy and operating efficiency of existing neural network models (Zhang *et al*., 2022) has gradually become one of the research hotspots. Hao *et al*., (2015) proposed a differential evolution ant colony wavelet neural network with relative entropy as the optimization standard and verified the accuracy of the model through the measured data of surface settlement during the shield construction of Beijing Metro Line 6, and achieved good results. There are still some imperfections in the neural network method itself. When the number of training samples is too small, the prediction accuracy cannot be guaranteed. When the number of training samples is too large, it is difficult to normalize the prediction results. Therefore, seeking a more economical, accurate and efficient prediction model for the surface settlement of shield construction is essential.

Tipping M. E. (2001a; 2001b) proposed Relevance Vector Machine (Relevance Vector Machine, RVM) on the basis of Support Vector Machine (Yao *et al*., 2013; Borthakur and Dey, 2020) (Support Vector Machine, SVM). RVM includes the advantages of SVM and improves the shortcomings of SVM. The kernel function has a large degree of freedom. and fewer parameters, the correlation vector of the model is reduced. It has the characteristics of high sparsity in probabilistic model. Therefore, improves the prediction efficiency and can better handle the regression problem. However, the RVM model is slightly insufficient in the screening of influencing factors and the determination of kernel function parameters, which affects the diagnostic accuracy and generalization ability of RVM.

Therefore, this paper introduces Principal Component Analysis (PCA) (Su et al., 2021; Wang et al., 2022) and Particle Swarm Optimization (PSO) methods (Marini and Walczak, 2015; Yan et al., 2022). PCA filters out the principal components by dimensionality reduction, and PSO optimizes the relevant parameters of the model to obtain the optimal parameters. Based on them, this paper establishes a PCA-PSO-RVM for shield construction surface settlement prediction model with the actual case study of shield construction of Beijing Metro Line 6, and obtains a non-mapping relationship between surface settlement and principal components.

Under the same conditions, the RVM model, the PCA-RVM model, the PSO-RVM model and the PCA-PSO-RVM model were all used to predict the settlement, and the results obtained by the various models were compared for assessment of the prediction accuracy, dispersion and balance degree analysis. The comparative analysis of the indicators determines the sensitivity of the influencing factors, verifies the accuracy and reliability of the PCA-PSO-RVM shield construction surface settlement prediction model proposed in this paper, and provides a new way to obtain the shield construction surface settlement.

2 PCA-PSO-RVM model related theory

2.1 Principle of PCA

PCA is a process of computing the principal components and using them to perform a change of basis on the data, sometimes using only the first few principal components and ignoring the rest. It is used in this paper to reduce the dimensions of the multiple influencing factors affecting the surface settlement of shield construction through PCA projection. Assuming that there are *n* samples in the data set of surface settlement, and each sample has *p* values of influencing factors, an *n*×*p* order matrix is constructed.

$$\boldsymbol{X}_{n\times p}=\begin{bmatrix} x_{11} & x_{12} & \cdots & x_{1p} \\ x_{21} & x_{22} & \cdots & x_{2p} \\ \vdots & \vdots & \ddots & \vdots \\ x_{n1} & x_{n2} & \cdots & x_{np} \end{bmatrix} \tag{1}$$

Among them, x_{n1} represents the first influencing factor affecting the surface settlement, and x_{np} represents the *p*th influencing factor.

(1) In order to avoid the error caused by the different dimensions of each influencing factor, it is necessary to standardize the original data.

$$x_{ij}^{*}=\frac{x_{ij}-\overline{x}_j}{\sqrt{Var(x_j)}}(i=1,\ldots,n;\ j=1,\ldots,p) \tag{2}$$

$$\overline{x}_j=\frac{1}{n}\sum_{i=1}^{n}x_{i}\left(i=1,\ldots,n;j=1,\ldots,p\right) \tag{3}$$

$$Var(x_j)=\frac{1}{n-1}\sum_{i=1}^{n}(x_{ij}-\overline{x}_j)^2 \quad \left(i=1,\ldots,n;j=1,\ldots,p\right) \tag{4}$$

In the formula, $\overline{x}_j$ and $Var(x_j)$ represent the sample mean and variance of the *j*th factor, respectively.

(2) Find the correlation coefficient matrix ***M***:

$$\boldsymbol{M}=\begin{bmatrix} m_{11} & m_{12} & \cdots & m_{1p} \\ m_{21} & m_{22} & \cdots & m_{2p} \\ \vdots & \vdots & \ddots & \vdots \\ m_{p1} & m_{p2} & \cdots & m_{pp} \end{bmatrix} \tag{5}$$

$$m_{ij}=\frac{\sum_{k=1}^{n}(x_{ki}-\overline{x}_i)(x_{kj}-\overline{x}_j)}{\sqrt{\sum_{k=1}^{n}(x_{ki}-\overline{x}_i)^2(x_{kj}-\overline{x}_j)^2}} \tag{6}$$

In the formula, $m_{ij} = m_{ji}, m_{ii} = 1 (i, j = 1, \ldots, p; k = 1, \ldots, n-1)$

(3) Find the eigenvalues and eigenvectors of $\boldsymbol{M}$:

According to the characteristic equation $|\boldsymbol{M} - \lambda \boldsymbol{I}| = 0$ of $\boldsymbol{M}$, use the Jacobi method to obtain the p eigenvalues $\lambda_j (j = 1, 2, \ldots, p)$ of $\boldsymbol{M}$, and arrange $\lambda_1 \geq \lambda_2 \geq \cdots \geq \lambda_p \geq 0$ according to the size, and obtain the corresponding orthogonal unitized eigenvector $\boldsymbol{e}_1, \boldsymbol{e}_2 \cdots \boldsymbol{e}_p$.

(4) Determine the number of principal components q:

The contribution rate of variance and the cumulative contribution rate of the top q factors are $\lambda_i / \sum_{i=1}^{p} \lambda_i$ and $\sum_{i=1}^{q} \lambda_i / \sum_{i=1}^{p} \lambda_i \, (i = 1, 2, \ldots, p)$, respectively. The number of principal components is selected according to the cumulative contribution rate. Generally, the cumulative contribution rate is greater than 85%, and the corresponding first q principal components contain the information provided by the p original factors.

(5) Find the principal components

The original influencing factor is $x_1, x_2, \ldots, x_p$, and the principal component after PCA dimensionality reduction is $y_1, y_2, \ldots, y_q (q \leq p)$.

$$\begin{cases} y_1 = c_{11} x_1 + c_{12} x_2 + \cdots c_{1p} x_p \\ y_2 = c_{21} x_1 + c_{22} x_2 + \cdots c_{2p} x_p \\ \vdots \\ y_q = c_{q1} x_1 + c_{q2} x_2 + \cdots c_{qp} x_p \end{cases} \tag{7}$$

In the formula, c_{ij} and y_i are uncorrelated, and $c_{i1}^2 + c_{i2}^2 + \cdots c_{ip}^2 = 1$. y_i is the one with the largest variance among all linear combinations of $x_1, x_2, \ldots, x_p$, and $y_1, y_2, \ldots, y_q$ is uncorrelated with each other, thus reducing the number of variables and achieving the effect of dimensionality reduction. The principle is shown in Fig. 1.

2.2 Principle of RVM

2.2.1 Model description

RVM (Ma and Hanson, 2020; Galuzio *et al.*, 2020) is a sparse probability model based on Bayesian principle proposed by American scholar Micnacl E. Tipping in 2000.As a new supervised learning method, it can train the model quickly. It uses the weighted combination of kernel functions to apply to regression and other problems. At the same time, machine learning based on Bayesian principle is used to ensure the sparsity of the model.

Let the training sample data set be $\{x_n, t_n \mid n = 1, 2, ..., N\}$, x_n represents the input training sample vector value, and t_n represents the output target value. Suppose t_n is independently distributed with Gaussian white noise ξ_n, and establish a functional relationship about t_n:

$$t_n = y(x_n; \boldsymbol{\omega}) + \xi_n \tag{8}$$

$$y(\boldsymbol{x}, \boldsymbol{\omega}) = \sum_{n=1}^{N} \omega_n K(\boldsymbol{x}, x_n) + \omega_0 \tag{9}$$

Among them, ω represents the weight vector, $\omega = [\omega_0, \omega_1, \ldots, \omega_N]^T$, $K(\boldsymbol{x}, x_n)$ represent the kernel function, and ω_0 is the bias. ξ_n represents the additional Gaussian noise satisfying $\xi_n \sim N(0, \sigma^2)$, and the variance σ^2 is an unknown quantity, which needs to be obtained by iteration. Because the Gaussian kernel function is stable and has strong linear interpolation ability, this paper uses the Gaussian kernel function.

$$K(\|y - y_c\|) = \exp\left\{-\frac{\|y - y_c\|^2}{2w^2}\right\} \tag{10}$$

where y_c is the center of the kernel function, and W is the width of the Gaussian kernel. Assuming that t_n are distributed independently of each other, the likelihood function of the dataset of training samples can be expressed as:

$$p(\boldsymbol{t} \mid \boldsymbol{\omega}, \sigma^2) = (2\pi\sigma^2)^{-N/2} \exp\{-\frac{1}{2\sigma^2}\|\boldsymbol{t} - \boldsymbol{\Phi\omega}\|^2\} \tag{11}$$

Among them, $\boldsymbol{t} = (t_1, \ldots, t_N)^{\mathrm{T}}$ is the target vector, $\boldsymbol{\omega} = [\omega_0, \omega_1, \ldots, \omega_N]^{\mathrm{T}}$ is the parameter vector, $\boldsymbol{\Phi}$ is the $N \times (N+1)$ matrix composed of the kernel function, and $\boldsymbol{\Phi} = [\boldsymbol{\phi}(x_1)\boldsymbol{\phi}(x_2)\ldots\boldsymbol{\phi}(x_N)]^{\mathrm{T}}$, $\boldsymbol{\phi}(x_n) = [1, K(x_n, x_1), K(x_n, x_2), \ldots, K(x_n, x_N)]^{\mathrm{T}}$. In order to avoid the occurrence of over-learning phenomena, certain mandatory conditions can be attached to some parameters.

The Bayesian perspective method is applied in the correlation vector machine, and the size of each weight parameter ω_n is set to zero mean in the Gaussian prior distribution, which constitutes a simple function about ω , and such a function is in the zero mean Gaussian. The prior distribution is widely used.

$$p(\omega|\alpha) = \prod_{n=0}^{N} N\,(\omega_n|0, \alpha_n^{-1}) \tag{12}$$

The parameters in the formula are all independently distributed, and the complexity of the prior function distribution has been greatly alleviated. α is the *N+1*-dimensional hyperparameter that determines the prior distribution of the weight ω, and the hyperparameter vector $\alpha = (\alpha_0, \alpha_1, \ldots, \alpha_N)$. In order to obtain the final function, the scale function parameter σ^2 also needs to be introduced.

2.2.2 Parameter inference and regression prediction

According to the prior probability distribution, the posterior probability distribution of the training samples can be worked out based on Bayesian theory.

$$P(\omega, \alpha, \sigma^2|t) = \frac{P(t|\omega,\alpha,\sigma^2)P(\omega,\alpha,\sigma^2)}{P(t)} \tag{17}$$

$$P(t) = \int P(t|\omega, \alpha, \sigma^2)\, P(\omega, \alpha, \sigma^2) d\omega d\alpha d\sigma^2 \tag{18}$$

Since the posterior probability distribution $P(\omega, \alpha, \sigma^2|t)$ cannot be directly calculated through integration, it is decomposed into

$$P(\omega, \alpha, \sigma^2|t) = P(\omega|t, \sigma, \sigma^2)P(\alpha, \sigma^2|t) \tag{19}$$

The posterior distribution of the available weight vector ω is:

$$P(\omega|t,\alpha,\sigma^2)=\frac{P(t|\omega,\sigma^2)P(\omega|\alpha)}{P(t|\alpha,\sigma^2)}=(2\pi)^{-(N+1)/2}|\Sigma|^{-1/2}exp\{-\frac{1}{2}(\omega-\mu)^T\Sigma^{-1}(\omega-\mu)\} \quad (20)$$

Among them, it can be concluded that the probability distribution obeys the multivariate Gaussian model, the posterior probability distribution mean $\mu=\sigma^{-2}\Sigma\Phi^T t$, the covariance $\Sigma=(\sigma^{-2}\Phi^T\Phi+A)^{-1}$ represents the uncertainty of the model prediction, and $A=diag(\alpha_0,\alpha_1,\ldots,\alpha_N)$ represents the diagonal matrix.

In the process of estimating hyperparameters, the maximum likelihood estimation parameters α_{MP} and σ^2_{MP} can be obtained according to parameter inference. Assuming that the sample to be tested is x^*, the predicted value t^* is distributed as follows:

$$P(t^*|t,\alpha_{MP},\sigma^2_{MP})=\int P(t^*|\omega,\sigma^2_{MP})\,P(\omega|t,\alpha_{MP},\sigma^2_{MP})d\omega \quad (21)$$

$$P(t^*|t,\alpha_{MP},\sigma^2_{MP})=N(t^*|y^*,\sigma^2_*) \quad (22)$$

Among them, expected value $y^*=\mu^T\phi(x^*)$, variance $\sigma^2_*=\sigma^2_{MP}+\phi(x^*)^T\sum\phi(x^*)$. Therefore, the distribution of the predicted value t^* of the sample x^* to be tested, the mean value $y^*=(x^*;\mu)$. In order to facilitate understanding, Fig. 2 shows the visual structure of the model, which contains the input layer, hidden layer and result output layer of the data.

2.3 Principle of Particle Swarm Optimization (PSO)

Kennedy and Eberhart proposed PSO in 1995 based on the simulation of bird flock foraging behavior. It is the use of particle swarm stochastic intelligence optimization characteristics, using the relationship between individuals and groups, through the individual particle swarm in the group of competition and cooperation generated by the group intelligence, and ultimately guide the optimization of search. PSO is widely used in pattern recognition and parameter optimization due to its advantages of less parameters, intelligent optimization, and fast convergence.

The particles in the PSO represent the answer to the problem to be solved, the coordinate vector $x_i = (x_1, x_2, ..., x_d, ..., x_D)$ of each particle, the flying speed $v_i = (v_{i1}, v_{i2}, ..., v_{id}, ..., v_{iD})$ of the particle, the historical optimal coordinate $P_i = (P_{i1}, P_{i2}, ..., P_{id}, ..., P_{iD})$ of the *i*th particle, the optimal coordinate $P_g = (P_{g1}, P_{g2}, ..., P_{gd}, ..., P_{gD})$ experienced by each particle, and the particle swarm is flying during the flight process. continuously updated.

$$v_{id}^{k+1} = \omega v_{id}^k + c_1 r_1 (P_{id} - x_{id}^k) + c_c r_2 (P_{gd} - x_{id}^k) \tag{23}$$

$$x_{id}^{k+1} = x_{id}^k + v_{id}^{k+1} (i = 1, 2, ..., m; d = 1, 2, ..., D) \tag{24}$$

Among them, *m* is the particle swarm size, *D* is the particle swarm dimension, v_{id}^k is the iteration offset, *k* is the number of iterations, ω is the inertia weight, c_1 and c_2 are the acceleration factors, and r_1 and r_2 are based on random number between [0,1]. The overall schematic diagram is shown in Fig. 3.

For the selection of the acceleration parameter, it is known from the literature (Wang and Ma, 2017) that in general c_1= c_2, which can be chosen as any constant between 1.8 and 2.0. In the manuscript, we define the acceleration parameter as c_1= c_1=2. For the choice of population size, the population size *N* is determined by the complexity of the problem. Too small a population size will make the results less accurate, while too large a population size will make the processing slower, computationally more expensive and time-consuming. A more appropriate value needs to be selected by synthesizing between the degree of accuracy and the cost effective. of calculation, which can be done by summarizing the existing references (Wen and Liu, 2004) and selecting the appropriate population size, so the population size *N*=20 is selected in this paper.

For the maximum number of iterations of the particle swarm algorithm, the larger the maximum number of iterations, the better, under the premise of satisfying the minimum error. Considering the existing literature, the maximum number of iterations chosen in this paper is M= 1000.

2.4 Comparison of the merits and demerits of the models

PCA can make RVM more efficient and convenient in analyzing sample data, and PSO makes the problem of kernel function parameters of RVM solved. The PCA-PSO-RVM model proposed in this paper is more advanced and computationally more powerful than the RVM model, PSO-RVM model and PCA -RVM model. The results of comparing the above models are shown in Table 1 below:

3 Building the predictive models

3.1 Background of the project

In this paper, the ground settlement data for the shield construction from East New Town Station to Dong Xiaoying Station of Beijing Metro Line 6 are used. The section of the interval passes through green areas and Songlang intersection along the line, where there are several rainwater, power and telecommunication pipelines at Songlang Road intersection and Canal East Street Southeast, with a total length of 842.95m. Shield construction interval tunnel design section is circular, the outer diameter is 6.0m, the inner diameter 5.4m, the ground elevation along the interval 19.5m to 19.8m, interval tunnel bottom buried depth 13.7m to 21m, through the stratum mainly includes a layer of fine powder sand, medium and coarse sand layer, local sandwich powder clay layer.

3.2 data samples

The surface settlement of shield construction is affected by the interaction of soil parameters and construction parameters, and there are often a series of problems such as uncertainty and randomness when selecting influencing factors. In this paper, PCA is used to reduce the dimension of multiple influencing factors to obtain new principal component variables, and then use the PSO-RVM model to predict.

Based on the analysis of soil characteristics and shield machine parameters during the actual construction of Beijing Metro Line 6, the jack thrust (F), grouting pressure (P), overburden thickness (H), weighted average compression modulus (Es), weighted average cohesion (C), weighted average natural density (ρ), and weighted average internal friction angle (φ), a total of seven conventional physical parameters, were comprehensively selected. These seven parameters were used as the relevant influencing factors of surface settlement (S), and the relevant data are shown in Table 2. Equation (6) was calculated for the seven influencing factors in the 51 sets of data after standardization in Table 2, and the correlation coefficient matrix was obtained as shown in Table 3.

It can be seen from Table 3 that the absolute values of the correlation coefficients between the seven influencing factors, such as jack thrust, grouting pressure, and covering soil thickness, are all between 0 and 1, and there is correlation between each factor, and the closer the correlation coefficient is to one factor. the greater the correlation. In order to further explore the specific influence value of each factor, the score diagram of 51 groups of data is obtained based on the PCA principle Fig. 4 (a), and the contribution rate and cumulative contribution rate of each factor are calculated Fig. 4 (b).

Fig. 4(b) shows that the contribution rate of jack thrust (F), grouting pressure (P) and covering soil thickness (H) is the largest, and the contribution rates of other influencing factors decrease in turn. The cumulative contribution rate of the first four influencing factors is 86.539% and exceeds 85%, indicating that it contains the amount of information represented by the seven factors. According to the cumulative contribution rate, four principal component variables are extracted. Each principal component variable is equal to the product of the seven influencing factors and their corresponding seven component score coefficients.

3.3 Surface settlement model of shield tunneling construction

In this paper, 7 influencing factors are dimensionality reduced into 4 principal component variables through PCA, and the 4 principal component variables are selected as the variable input layer of the shield construction surface settlement, and the surface settlement is used as the output layer. The optimal parameters were automatically retrieved through PSO, and then a PCA-PSO-RVM correlation model based on four principal component variables was established according to the principle of the PCA-PSO-RVM regression prediction model.

3.4 prediction steps

（1）The input data of the sample is the four principal components of the surface settlement of the shield construction, and the output data is the surface settlement, and the influencing factors are standardized.

（2）Initialize the position and velocity of the particle swarm, determine the size of the particle swarm, and update the parameters of the PSO model according to the formula.

（3）It is judged whether the termination condition is met, and the optimal kernel function parameters of the RVM model are further calculated, and the PSO-RVM prediction model is established.

（4）The predicted value and the corresponding measured value are compared and analyzed for multiple indicators to verify the accuracy and reliability of the model. The overall process is shown in Fig. 5.

4 Validation

In this paper, the four principal component variables processed by PCA and the relevant data of surface settlement are used to verify the accuracy of the PSO-RVM prediction model, and the optimal solution is found after many times of learning. The prediction results of PCA-PSO-RVM model and RVM model, PCA-RVM model and PSO-RVM model in surface settlement were compared under the same sample conditions, as shown in Table 4.

It can be seen from Table 4 that in the relative error of the PCA-PSO-RVM machine model, the smallest sample No. 51 and No. 46 are only 0.06%, while in the PSO-RVM, PCA-RVM and RVM models, the minimum relative errors are 0.21%, 0.56%, 0.97%. In the comparison of the maximum relative error, the prediction error of the PCA-PSO-RVM model is also the smallest, only 0.73%. The overall analysis PCA-PSO-RVM model is the most accurate, and Fig. 6 more intuitively shows the distribution characteristics of the prediction results of the four models.

It can be seen from Fig. 6 that the prediction results of PCA-PSO-RVM are closer to the true value than the prediction results of the PSO-RVM model, the prediction results of the PCA-RVM model and the RVM model, and the fitting degree is significantly higher than that of the other three prediction models. The predicted value of each sample of the RVM model has the largest dispersion, especially the predicted value of No. 46, 47 and 50 samples obviously deviates from the measured value. In order to better compare the overall prediction accuracy, dispersion and balance of the four models, the average relative error MRE, root mean square error RMSE, and Theil inequality coefficient TIC of the four models were calculated respectively (Murray_smith, 1998). Calculated as follows:

$$\mathrm{MRE} = \frac{1}{n}\sum_{i=1}^{N}\frac{|y_i - y_i'|}{y_i} \times 100\% \tag{27}$$

$$\mathrm{RMSE} = \sqrt{\frac{1}{n}\sum_{i=1}^{n}(y_i - y_i')^2} \tag{28}$$

$$\mathrm{TIC} = \frac{\sqrt{\frac{1}{n}\sum_{i=1}^{n}(y_i - y_i')^2}}{\sqrt{\sum_{i=1}^{n} y_i^2} + \sqrt{\sum_{i=1}^{n}(y_i')^2}} \tag{29}$$

Among them, n is the number of samples; y_i is the actual monitoring value; y_i' is the model predicted value. The specific distribution of the average relative error MRE, the root mean square error RMSE, and the Theil inequality coefficient TIC is shown in Fig. 7.

Fig. 7(a) highlights the comparison of the degree of error of the models. The average relative errors of PCA-PSO-RVM and PSO-RVM are 0.17% and 1.25%, while the average relative errors of PCA-RVM model and RVM model are 1.63% and 3.76%. The relative degree of PCA-PSO-RVM is the smallest. Fig. 7(b) highlights the dispersion of the model prediction results, the rms of PCA-PSO-RVM and PSO-RVM are 0.0714 and 0.4744, and the PCA-RVM model and RVM model are 0.5981 and 1.9184. Fig. 7(c) highlights the degree of balance of the model prediction results, with the Theil inequality coefficients of 0.027% and 0.183% for PCA-PSO-RVM and PSO-RVM, 0.231% and 0.775% for PCA-RVM model and RVM model, PCA-PSO-RVM has the least volatility. The comparison of the calculation results of the three indices shows that the PCA-PSO-RVM model has a greater advantage. The PCA-PSO-RVM model proposed in this paper has higher overall prediction accuracy, less discreteness and higher reliability.

5 Sensitivity analysis

Jack thrust (*F*), grouting pressure (*P*), overburden thickness (*H*), weighted average compression modulus (*E*s), weighted average cohesion (*C*), weighted average natural density (ρ) and weighted average internal friction angle (φ) affect the surface settlement of shield tunneling in varying degrees. In order to explore the sensitivity of the seven influencing factors, on the basis of MRE, RMSE and TIC calculated by each prediction model, the impact degree of the factors is evaluated and compared, which is helpful for researchers to determine and pay attention to the parameters of surface settlement during shield construction. The formula is as follows:

$$\mathrm{R}_{1j} = \mathrm{MRE}_j / \mathrm{MRE} \tag{30}$$

$$\mathrm{R}_{2j} = \mathrm{RMSE}_j / \mathrm{RMSE} \tag{31}$$

$$\mathrm{R}_{3j} = \mathrm{TIC}_j / \mathrm{TIC} \tag{32}$$

In the formula, R_{1j}, R_{2j}, R_{3j} are the ratios of the three indicators (MRE, RMSE and TIC), respectively, and the results obtained by the new model are compared with those obtained by the original model. The value of j (=1, 2,…,7) corresponds to the seven influencing factors (*F, P, H*, E_s, *C*, ρ and φ) not considered by the new model in turn, RMSE, TIC, and MRE are the missing *j*th factor, respectively. Standard deviztion, root mean square error, and Theil inequality coefficient. MRE_j, RMSE_j, and TIC_j represent the three indicators of the initial prediction model, respectively. The size of R_{ij} is proportional to the sensitivity of surface settlement.

Table 5 shows the calculated values of the three indicators of the model prediction results without corresponding factors, as well as the comparison results of the three indicators. Compared with the calculation results of Fig. 7, the three indicators calculated by the six-factor model are all larger than the indicators calculated by the original model, emphasizing the importance of the 7-factor model and paving the way for easy identification of the sensitivity of the factors. The comparison values of the three indicators are all greater than 1, indicating that each factor will affect the prediction results of Surface settlement to varying degrees. The ranking of sensitive factors further compares the degree of influence of the factors. The above shows that the seven factors selected in this paper are reasonable. In order to intuitively show the influence of each factor on the surface settlement, the radar chart in Fig. 8 is used to represent the distribution of multiple indicators.

The size of the radar chart reflects the quality of the evaluation object, which can be used as a basis to diagnose and control the evaluation object. For indicators that are closer to the center, the more measures to be taken to improve. It can be seen that F, P, H, Es and C are the closest to the center, and corresponding measures should be taken in the study of the surface settlement of shield construction. Among the factors affecting the surface settlement, the weighted average natural density (ρ) and the weighted average internal friction angle (φ) have the largest sensitivity factor index to the surface settlement of shield construction, indicating that these two factors are closely related to the surface settlement. Then the jack thrust (F), grouting pressure (P), soil cover thickness (H), weighted average compressive modulus (E_s) and weighted average cohesion (C) need to be improved in the study.

6 Conclusion

Establishing an accurate prediction model for the surface settlement of shield construction can help control the shield construction process and reduce the adverse effects of surface settlement caused by the construction process. Based on the shield construction data of Beijing Metro Line 6, a PCA-PSO-RVM prediction model is established. The main conclusions are as follows:

(1) The surface settlement of shield tunneling is affected by multiple factors, and there is an intricate nonlinear mapping relationship between each factor and the surface settlement. The PCA-PSO-RVM prediction model proposed in this paper can accurately establish the nonlinear mapping relationship between surface settlement and influencing factors, simplify complex problems and facilitate the establishment of prediction models.

(2) Examples show that the prediction of surface settlement for shield construction using the PCA-PSO-RVM model yields better results than the RVM model, PCA-RVM model and PSO-RVM model, and that the PCA-PSO-RVM model has a clear advantage for problems with a small number of learning samples for prediction. The 7 influencing factors were reduced into 4 linearly independent principal components by PCA, and the redundant information among the influencing factors was eliminated. Through sensitivity factor analysis, the precise sensitivity and discrete sensitivity of the main influencing factors are further understood, and it is known that the weighted average internal friction angle (φ) has the greatest influence among the influencing factors.

(3) In the field inspection, combined with the method proposed in this study, the RVM model can be used to collect more extensive information to screen out the factors that have a greater impact on the surface settlement of shield construction, and to summarize a more complete nonlinear mapping relationship. Then a more optimized PCA-PSO-RVM model is obtained, which improves the accuracy and applicability of model prediction. At the same time, the parameters and influencing factors can be adjusted reasonably according to the actual problems in the shield construction site and the valuable opinions put forward by the researchers, so that the model has a wider scope of application.

7 Data Availability

Some or all data, models, or code that support the findings of this study are available from the corresponding author upon reasonable request.

8 Acknowledgements

The authors would like to acknowledge the financial support from the National Natural Science Foundation of China under Grant No.52068016. The work in this paper was also supported by the Guangxi Key Laboratory of Geomechanics and Geotechnical Engineering (Grant No.19-Y-21-9, 20-Y-XT-01), the High Level Innovation Team and Outstanding Scholar Program of Universities in Guangxi Province. (Grant No. 202006) and the Guangxi Natural Science Foundation under Grant Nos. 2020GXNSFAA297118 and 2020GXNSFAA159125.

References:

Azhdar, R. and Nazemi, A. (2020) Modeling of incentive-based policies for demand management for the Tehran subway. *Travel Behaviour and Society* **20**: 174-180, https://doi.org/10.1016/j.tbs.2020.03.014.

Borthakur, N. and Dey, A. (2020) Evaluation of Group Capacity of Micropile in Soft Clayey Soil from Experimental Analysis Using SVM-Based Prediction Model. *International Journal of Geomechanics* **20(3)**: https://doi.org/10.1061/(ASCE)GM.1943-5622.0001606.

Chou, W. and Bobet, A. (2002) Predictions of ground deformations in shallow tunnels in clay. *Tunnelling and Underground Space Technology* **17(1)**: 3-19, https://doi.org/10.1016/S0886-7798(01)00068-2.

Chen, R., Zhang, P., Kang, X., Zhong, Z., Liu, Y. and Wu, H. (2019) Prediction of maximum surface settlement caused by earth pressure balance (EPB) shield tunneling with ANN methods. *Soils and Foundations* **59(2)**: 284-295, https://doi.org/10.1016/j.sandf.2018.11.005.

Du, R. and Zheng, S. (2020) Agglomeration, housing affordability, and new firm formation: The role of subway network. *Journal of Housing Economics* **48**: 101668, https://doi.org/10.1016/j.jhe.2020.101668.

Galuzio, P., de Vasconcelos Segundo, E., Coelho, L. and Mariani, V. (2020) MOBOpt — multi-objective Bayesian optimization. *SoftwareX* **12**: 100520, https://doi.org/10.1016/j.softx.2020.100520.

Hao, R., Ji, Y. and Ni, Z. (2015) Study on predicting the surface settlement for shield tunneling based on DEACO－WNN. *Journal of Railway Engineering Society* **32(1)**: 12-16.

Kasper, T. and Meschke, G. (2006) On the influence of face pressure, grouting pressure and TBM design in soft ground tunnelling. *Tunnelling and Underground Space Technology* **21(2)**: 160-171, https://doi.org/10.1016/j.tust.2005.06.006.

Kennedy, J. and Eberhart, R. (1995) Particle swarm optimization. *Proceedings of ICNN'95 - International Conference on Neural Networks. IEEE.* **4:** 1942-1948, https://doi.org/10.1109/ICNN.1995.488968

Li, S. H., Zhang, M. J., and Li, P. F. (2021) nalytical solutions to ground settlement induced by ground loss and construction loadings during curved shield tunneling. *Journal of Zhejiang University-SCIENCE A*, ***22*****(4)**, 296-313，https://doi.org/10.1631/jzus.A2000120

Liu, B., Yu, Z., Han, Y., Wang, Z., Zhang, R. and Wang, S. (2020) Analytical solution for the response of an existing tunnel induced by above-crossing shield tunneling. *Computers and Geotechnics* **124**: 103624, https://doi.org/10.1016/j.compgeo.2020.103624.

Murray_smith, D. (1998) Methods for the external validation of contiuous system simulation models:a review.

Mathematical and Computer Modelling of Dynamical Systems **4(1)**: 5-31, https://doi.org/10.1080/13873959808837066.

Marini, F. and Walczak, B. (2015) Particle swarm optimization (PSO). A tutorial. *Chemometrics and Intelligent Laboratory Systems* **149**: 153-165, https://doi.org/10.1016/j.chemolab.2015.08.020.

Ma, Z. and Hanson, T. (2020) Bayesian nonparametric test for independence between random vectors. *Computational Statistics & Data Analysis* **149**: 106959, https://doi.org/10.1016/j.csda.2020.106959.

Ocak, I. and Seker, S. (2013) Calculation of surface settlements caused by EPBM tunneling using artificial neural network, SVM, and Gaussian processes. *Environmental Earth Sciences* **70(3)**: 1263-1276, https://doi.org/10.1007/s12665-012-2214-x.

Peck, R. B. (1969) Deep excavations and tunneling in soft ground. Proceeding of 7th international conference on soil mechanics and foundation engineering. *Mexico City: State of the Art Report:* 225-290.

Salimi, A., Rostami, J., Moormann, C. and Delisio, A. (2016) Application of non-linear regression analysis and artificial intelligence algorithms for performance prediction of hard rock TBMs. *Tunnelling and Underground Space Technology* **58**: 236-246, https://doi.org/10.1016/j.tust.2016.05.009.

Sharghi, M., Chakeri, H. and Ozcelik, Y. (2017) Investigation into the effects of two component grout properties on surface settlements. *Tunnelling and Underground Space Technology* **63**: 205-216, https://doi.org/10.1016/j.tust.2017.01.004.

Singh, D., Aromal, V. and Mandal, A. (2018) Prediction of surface settlements in subway tunnels by regression analysis. *International Journal of Geotechnical Engineering* **14(7)**: 836-842, https://doi.org/10.1080/19386362.2018.1477294.

Su, M., Liu, Y., Xue, Y., Cheng, K., Ning, Z., Li, G. and Zhang, K. (2021) Detection method of karst features around tunnel construction by multi-resistivity data-fusion pseudo-3D-imaging based on the PCA approach. *Engineering Geology* **288**: 106127, https://doi.org/10.1016/J.ENGGEO.2021.106127.

Tipping, M.(2001) Sparse Bayesian learning and the relevance vector machine. *Journal of Machine Learning Research* **1(3)**: 211-244.

Tipping, M.(2001) The relevance vector machine. *Advances in Neural Information Processing Systems* **(12)**: 652-658.

Verruijt, A. and Booker, J. (1998) Surface settlements due to deformation of a tunnel in an elastic half plane. *Géotechnique* **48(5)**: 709-713, https://doi.org/10.1680/geot.1998.48.5.709.

Wang, F., Gou, B. and Qin, Y. (2013) Modeling tunneling-induced ground surface settlement development using a wavelet smooth relevance vector machine *Computers and Geotechnics* **54**: 125-132.

Wang, G. and Ma, Z. (2017) Hybrid particle swarm optimization for first-order Reliability Method. *Computers and Geotechnics*, **81:** 49–58, https://doi.org/10.1016/j.compgeo.2016.07.013.

Wang, J., Mohammed, A., Macioszek, E., Ali, M., Ulrikh, D. and Fang, Q., (2022) A Novel Combination of PCA and Machine Learning Techniques to Select the Most Important Factors for Predicting Tunnel Construction Performance. *Buildings* **12(7)**: 919, https://doi.org/10.3390/BUILDINGS12070919.

Wen, Z. and Liu, Y. (2004) Reactive power optimization based on PSO in a practical power system. *IEEE Power Engineering Society General Meeting, 2004*, 239-243, https://doi.org/10.1109/pes.2004.1372792.

Yao, Y., Liu, Y., Yu, Y., Xu, H., Lv, W., Li, Z. and Chen, X. (2013) K-SVM: An Effective SVM Algorithm Based on K-means Clustering. *Journal of Computers* **8(10)**: 2632-2639, https://doi.org/10.4304/jcp.8.10.2632-2639.

Yan, H., Liu, K., Xu, C. and Zheng, W. (2022) A novel method for identifying geomechanical parameters of rock masses based on a PSO and improved GPR hybrid algorithm. *Scientific Reports* **12(1)**:1-18, https://doi.org/10.1038/s41598-022-09947-7.

Zhou, C., Kong, T., Zhou, Y., Zhang, H. and Ding, L. (2019) Unsupervised spectral clustering for shield tunneling machine monitoring data with complex network theory. *Automation in Construction* **107**: 102924, https://doi.org/10.1016/j.autcon.2019.102924.

Zhang, W., Li, H., Wu, C., Li, Y., Liu, Z. and Liu, H. (2021) Soft computing approach for prediction of surface settlement induced by earth pressure balance shield tunneling. *Underground Space* **6(4)**: 353-363, https://doi.org/10.1016/j.undsp.2019.12.003.

Zhang, W., Gu, X., Tang, L., Yin, Y., Liu, D. and Zhang, Y. (2022) Application of machine learning, deep learning and optimization algorithms in geoengineering and geoscience: Comprehensive review and future challenge. *Gondwana Research* **109**: 1-17, https://doi.org/10.1016/j.gr.2022.03.015.

Table 1. Comparison of the merits and demerits of the models

Name of algorithm	RVM	PCA—RVM	PSO—RVM	PCA—PSO—RVM
Merits	The operational efficiency of the kernel function is improved and the sparsity is enhanced. Reduced for the number of sample data, suitable for small sample data prediction.	The complexity of the raw data is reduced and the overall speed and accuracy of the model is improved compared to RVM. It can quickly find the focus for the analysis of data with multiple influencing factors.	As a probabilistic global optimization algorithm, there are more opportunities to solve the global optimal solution. The kernel function parameter problem of RVM is solved and the model reliability is enhanced.	The model has strong universality and fast convergence. The influence of data samples and RVM kernel function parameters on the calculation results is reduced, and the overall accuracy and running speed are increased.
Demerits	The choice of kernel function parameters has a large impact on the results.	There are some limitations in using PCA for eigenvalue decomposition, such as the transformation matrix must be a square matrix. Kernel function parameters have great influence on the results.	For functions with multiple local extreme points, it is easy to fall into local extreme points.	The data samples should not be selected too small, otherwise overfitting may occur.

Table 2. Surface settlement for shield tunneling data set

Sample no.	F (kN)	P (MPa)	H (m)	E_s (MPa)	C (kPa)	ρ $(g \cdot cm^{-3})$	φ (∘)	S (mm)
1	18600	0.20	13.60	15.50	8.60	1.84	29.20	-19.70
2	22000	0.19	14.70	14.20	7.20	1.79	24.30	-26.70
3	24600	0.19	15.30	13.30	8.10	1.74	22.50	-11.20
4	17100	0.19	18.20	19.30	26.80	1.78	22.10	-26.30
5	18900	0.18	16.20	13.50	8.80	1.75	22.40	-37.60
6	16100	0.21	13.50	15.40	8.80	1.80	29.30	-69.30
7	21500	0.20	13.10	19.20	11.90	1.90	31.60	-58.00
8	21200	0.19	21.00	29.40	5.30	1.75	37.60	-4.80
9	17700	0.19	19.30	15.60	9.70	1.95	37.80	-25.40
10	15100	0.18	18.80	10.80	20.40	1.70	18.40	-34.10
11	22200	0.18	19.80	38.30	7.60	1.85	39.10	-45.90
12	21800	0.19	14.30	17.60	9.40	1.80	25.10	-22.70
13	21300	0.22	14.60	24.80	13.40	1.90	26.20	-30.20
14	17100	0.20	23.20	41.30	2.90	1.75	41.30	-2.30
15	17900	0.19	18.50	20.40	35.80	1.64	20.60	-25.50
16	16100	0.21	19.10	13.80	7.60	1.74	35.30	-50.10
17	20500	0.20	16.70	10.30	20.20	1.66	18.10	-39.50
18	24800	0.22	15.60	40.40	51.20	1.80	23.10	-14.30
19	19200	0.20	16.50	20.80	35.40	1.70	20.20	-20.90
20	14600	0.19	13.40	19.10	11.30	1.90	31.40	-7.71
21	17600	0.19	15.10	16.20	15.80	1.75	23.10	-15.80
22	20600	0.20	17.30	13.10	7.40	1.75	35.20	-35.60
23	20800	0.19	16.20	9.30	9.20	1.60	19.80	-27.10
24	21800	0.21	14.10	24.30	13.80	1.90	26.20	-22.20
25	19400	0.20	16.50	22.00	22.30	1.80	24.40	-33.50
26	17100	0.21	21.20	47.60	3.90	1.85	43.20	-3.70
27	21200	0.20	21.60	25.10	3.20	1.70	33.30	-47.10
28	17500	0.19	17.90	14.60	12.40	1.65	20.60	-33.30
29	23800	0.20	15.90	16.50	20.40	1.70	21.40	-29.70
30	20600	0.21	22.90	47.20	3.80	1.85	43.20	-4.90
31	22900	0.19	14.40	17.80	9.80	1.80	25.70	-24.50
32	21900	0.22	13.80	12.30	6.40	1.75	28.10	-9.70
33	25300	0.19	14.90	46.80	43.50	1.90	25.50	-20.80
34	18200	0.21	17.00	15.30	9.80	1.85	37.60	-37.60
35	19000	0.19	17.60	11.80	5.30	1.70	29.30	-35.20
36	20600	0.19	20.50	41.80	3.20	1.75	41.80	-5.30
37	21000	0.20	21.00	23.60	4.80	1.75	30.50	-57.20
38	21800	0.21	14.10	18.50	10.40	1.80	33.20	-55.60
39	16600	0.21	19.40	12.80	6.40	1.75	35.20	-39.30
40	18800	0.20	13.60	14.00	7.20	1.80	30.10	-43.70
41	24800	0.22	15.40	39.80	49.10	1.80	23.40	**-16.50***
42	22100	0.19	15.20	15.80	8.80	1.80	28.80	**-44.10***
43	20100	0.19	16.40	9.80	8.30	1.65	20.40	**-27.50***
44	18200	0.21	16.80	13.30	9.00	1.75	22.80	**-39.20***
45	21100	0.22	14.90	25.10	14.00	1.85	25.50	**-29.20***
46	21300	0.20	13.80	18.60	12.50	1.90	33.60	**-69.30***
47	15300	0.19	12.90	17.40	11.80	1.90	35.10	**-54.70***
48	16600	0.21	13.80	16.60	10.80	1.83	28.50	**-23.30***
49	21800	0.19	14.50	15.60	7.80	1.85	25.10	**-34.80***
50	21300	0.20	15.80	10.40	20.90	1.70	18.40	**-39.50***
51	16600	0.21	13.90	15.90	10.00	1.85	29.60	**-20.20***

Table 3. Correlation coefficient matrix

	F	P	H	E_s	C	ρ	φ
F	1.000	0.099	-0.148	0.287	0.304	0.020	-0.196
P	0.099	1.000	-0.127	0.200	0.150	0.226	0.140
H	-0.148	-0.127	1.000	0.438	-0.206	-0.313	0.450
E_s	0.287	0.200	0.438	1.000	0.257	0.332	0.480
C	0.304	0.150	-0.206	0.257	1.000	-0.038	-0.512
ρ	0.020	0.226	-0.313	0.332	-0.038	1.000	0.462
φ	-0.196	0.140	0.450	0.480	-0.512	0.462	1.000

Table 4. Prediction results of different methods

Sample no.	Measured value (m/s)	RVM		PCA-RVM		PSO-RVM		PCA-PSO-RVM	
		Predictive value (mm)	Relative error (%)	Predictive value (mm)	Relative error (%)	Predictive value (mm)	Relative error (%)	Predictive value (mm)	Relative error (%)
41	-16.50	-15.815	4.15	-16.267	1.41	-16.465	0.21	-16.556	0.34
42	-44.10	-43.509	1.34	-43.606	1.12	-43.725	0.85	-44.070	0.07
43	-27.50	-26.810	2.51	-27.346	0.56	-27.016	1.76	-27.298	0.73
44	-39.20	-37.487	4.37	-40.027	2.11	-39.757	1.42	-39.170	0.08
45	-29.20	-28.082	3.83	-28.654	1.87	-28.567	2.17	-29.132	0.23
46	-69.30	-65.031	6.16	-68.392	1.31	-68.565	1.06	-69.256	0.06
47	-54.70	-51.533	5.79	-54.005	1.27	-54.164	0.98	-54.663	0.07
48	-23.30	-22.543	3.25	-22.762	2.31	-22.988	1.34	-23.276	0.10
49	-34.80	-34.462	0.97	-34.490	0.89	-35.023	0.64	-34.769	0.09
50	-39.50	-37.110	6.05	-40.187	1.74	-39.014	1.23	-39.470	0.08
51	-20.20	-19.608	2.93	-19.517	3.38	-19.778	2.09	-20.187	0.06

Table 5. Sensitive factor comparison result

Research object		F	P	H	E_s	C	ρ	φ
Indicators	MRE(%)	0.20	2.20	0.21	1.20	0.95	5.23	8.23
	RMSE	0.082	0.712	0.099	0.476	0.308	2.068	3.217
	TIC(%)	0.032	0.275	0.038	0.182	0.119	0.804	1.189
Ratio	R_{1j}	1.18	12.94	1.24	7.06	5.59	30.76	48.41
	R_{2j}	1.15	9.97	1.39	6.67	4.31	28.96	45.06
	R_{3j}	1.19	10.19	1,41	6.74	1.61	10.86	16.07
Sensitivity factor order		7	3	6	4	5	2	1

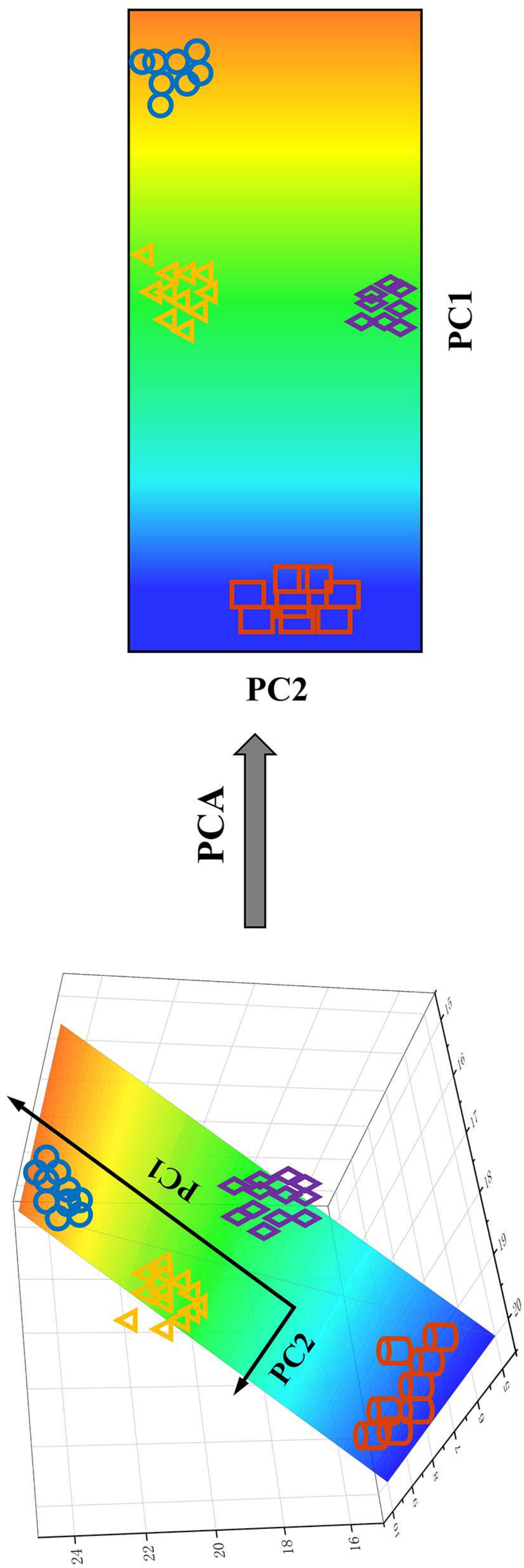
PC1
PC2
PCA
PC1
PC2
24
22
20
18
16
15
16
17
18
19
20

Figure

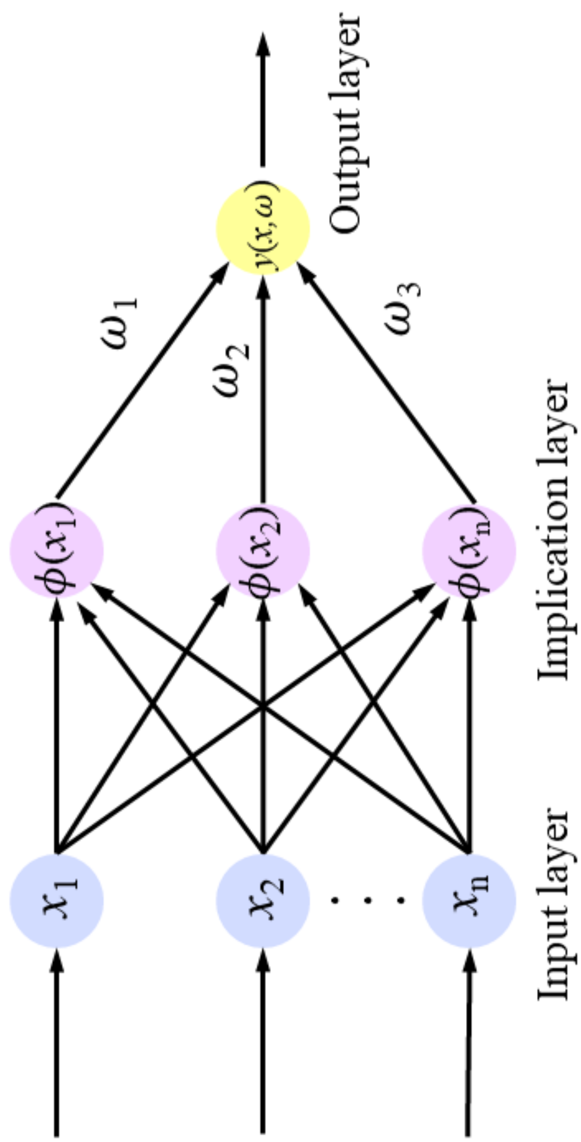

Output layer
Implication layer
Input layer
$y(x,\omega)$
ω_1
ω_2
ω_3
$\phi(x_1)$
$\phi(x_2)$
$\phi(x_n)$
x_1
x_2
x_n

Figure

Click here to access/download;Figure;Fig. 3. A schematic of PSO.eps

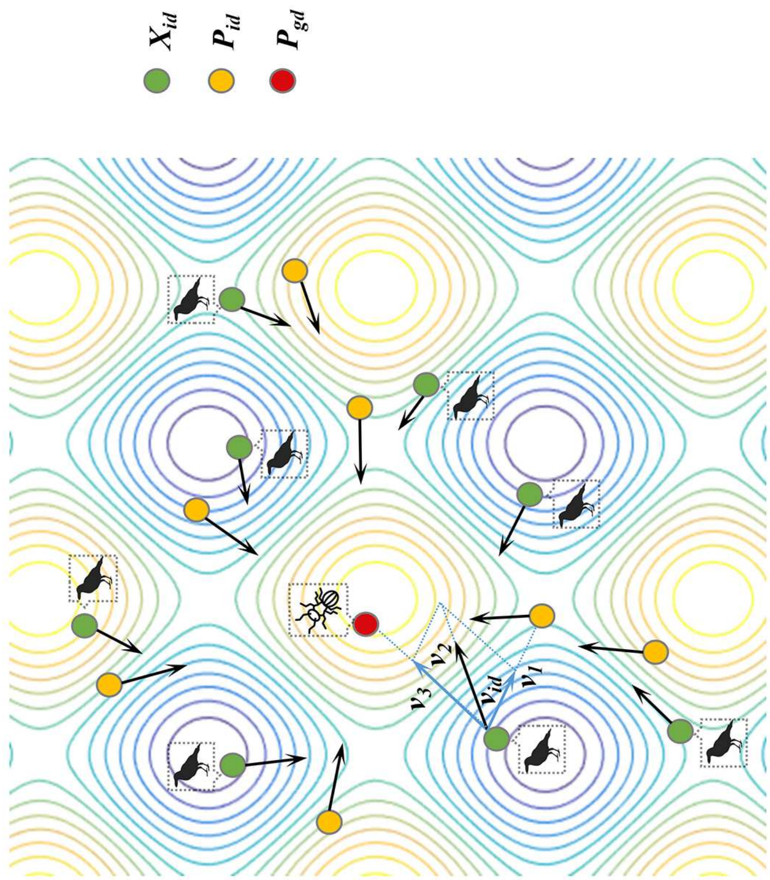

Figure

Click here to access/download;Figure;Fig. 4. PCA results and analysis process (a).eps

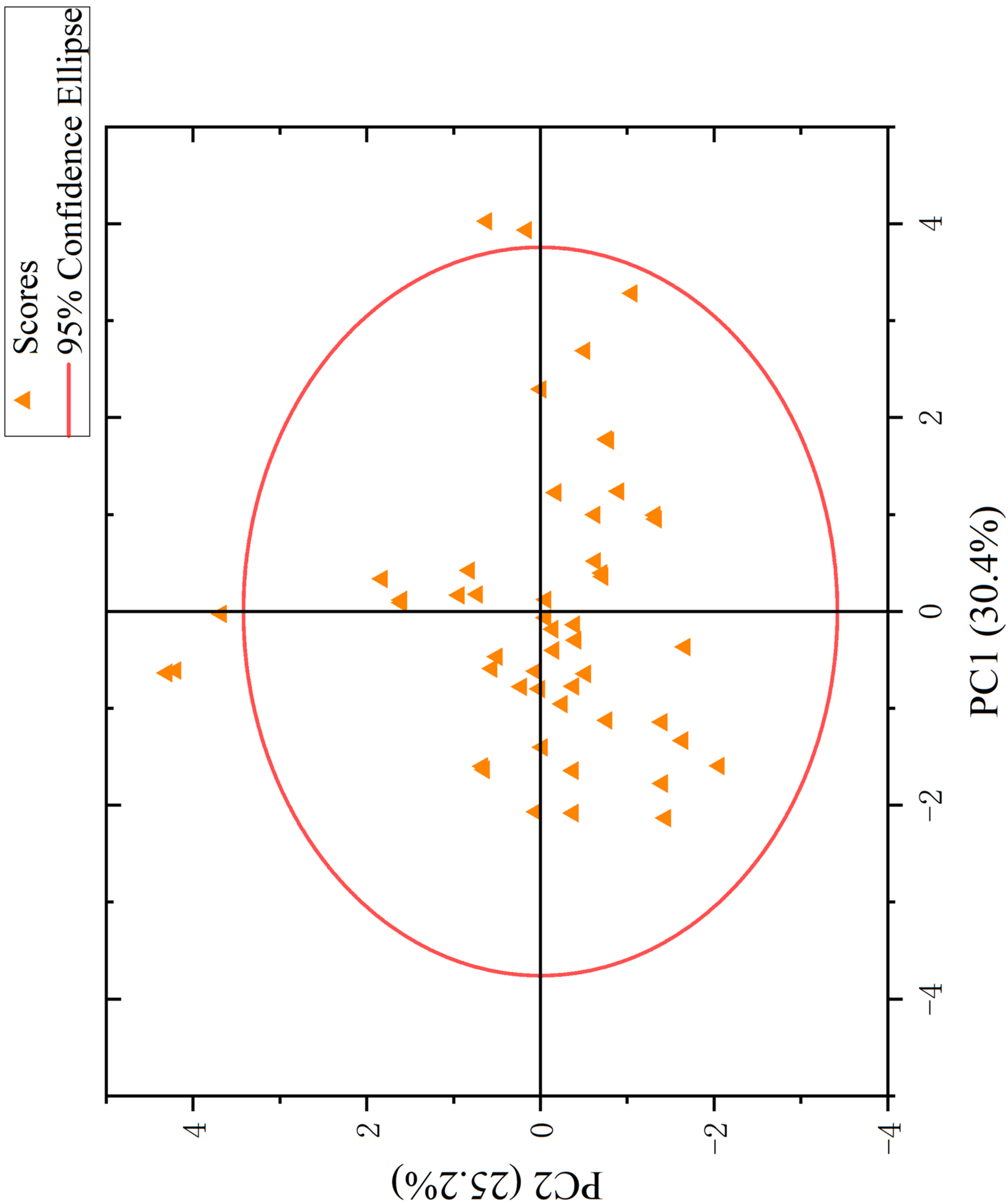

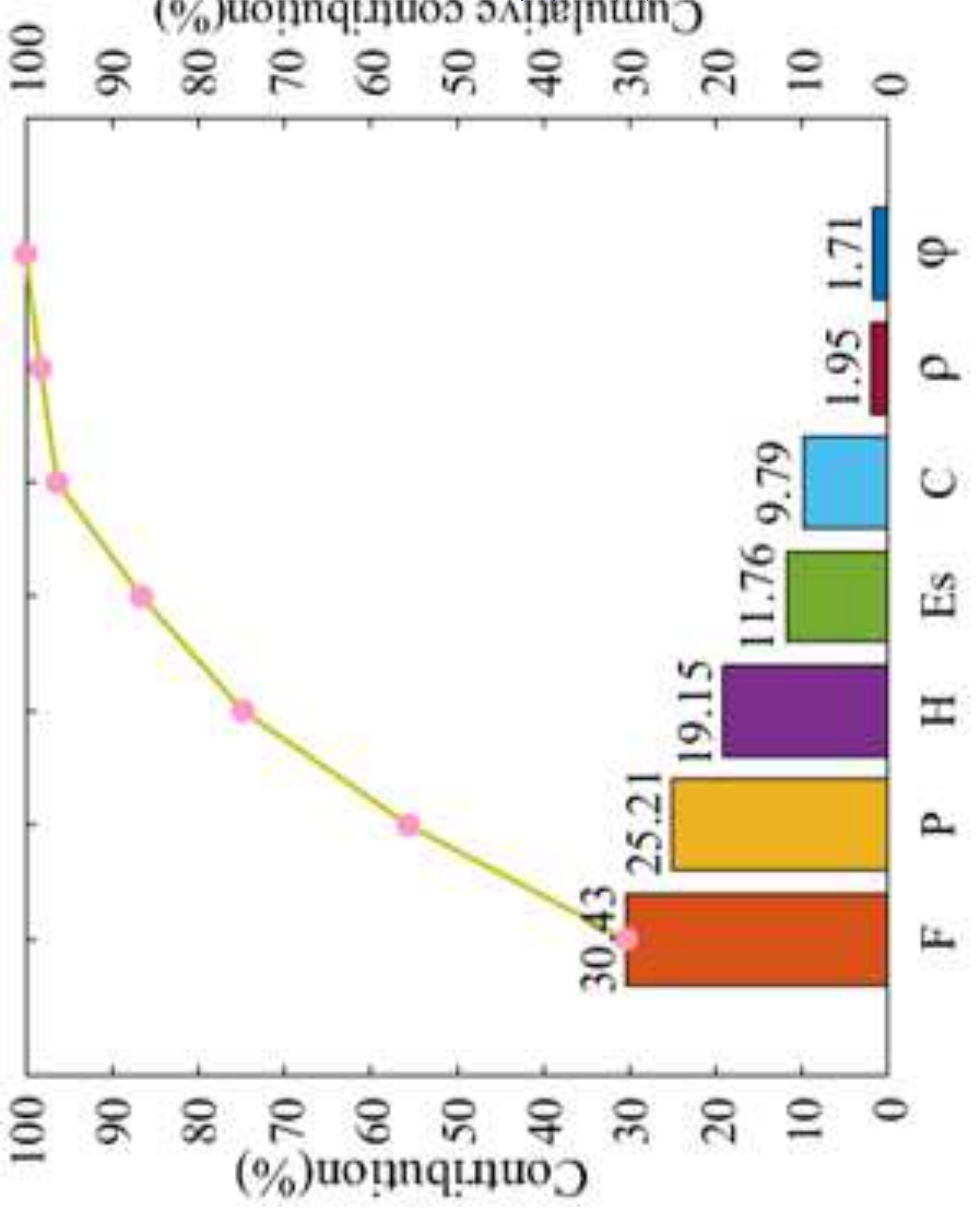
Cumulative contribution(%)
Contribution(%)
0
10
20
30
40
50
60
70
80
90
100
30.43
25.21
19.15
11.76
9.79
1.95
1.71
F
P
H
Es
C
ρ
φ

Figure

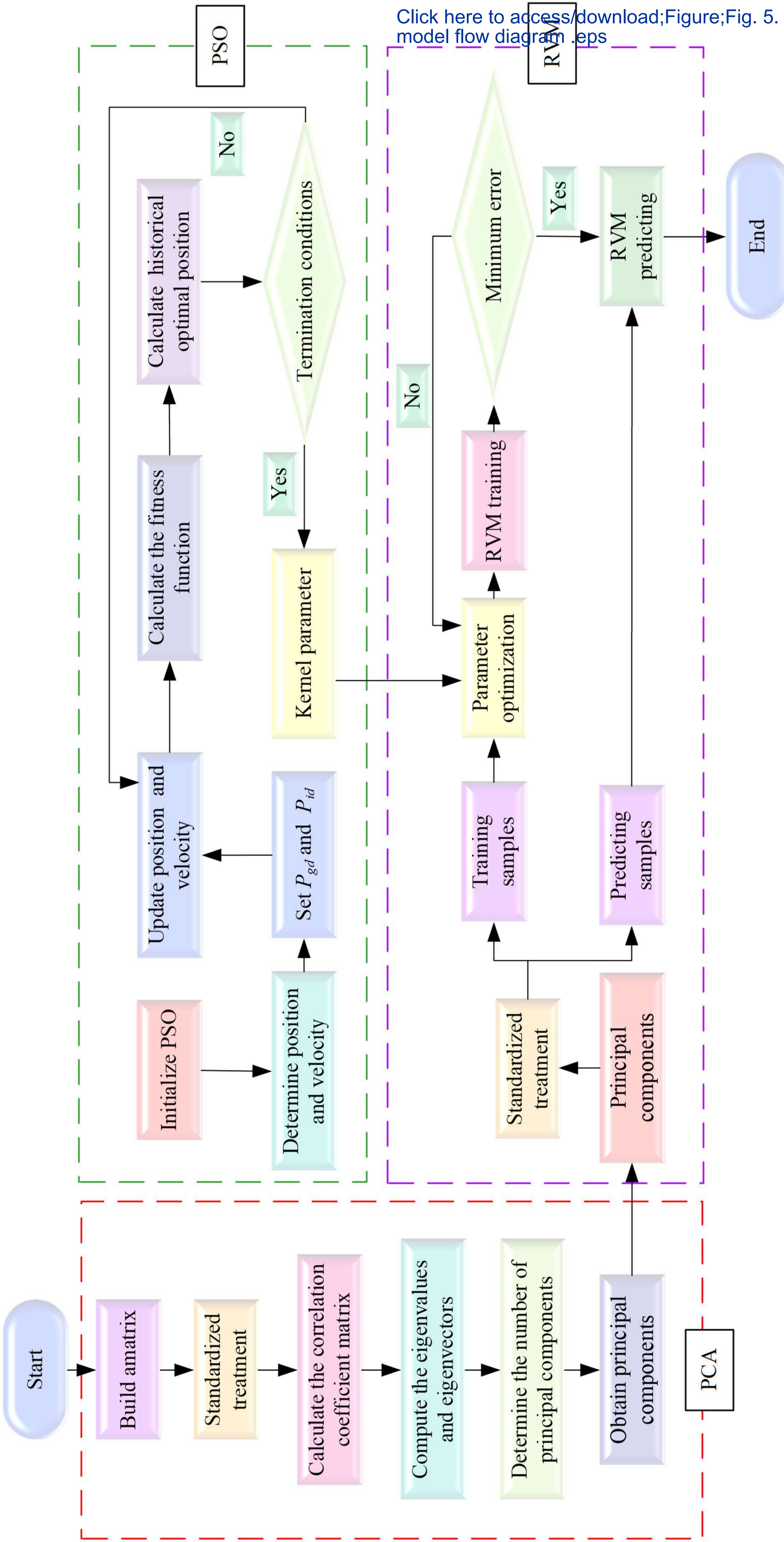

Start
PCA
Build amatrix
Standardized treatment
Calculate the correlation coefficient matrix
Compute the eigenvalues and eigenvectors
Determine the number of principal components
Obtain principal components
PSO
Initialize PSO
Determine position and velocity
Set P_{gd} and P_{id}
Update position and velocity
Calculate the fitness function
Calculate historical optimal position
Termination conditions
No
Yes
Kernel parameter
RVM
Principal components
Standardized treatment
Training samples
Predicting samples
Parameter optimization
RVM training
Minimum error
No
Yes
RVM predicting
End

Figure

Click here to access/download;Figure;Fig. 6. Different methods for predicting results.eps

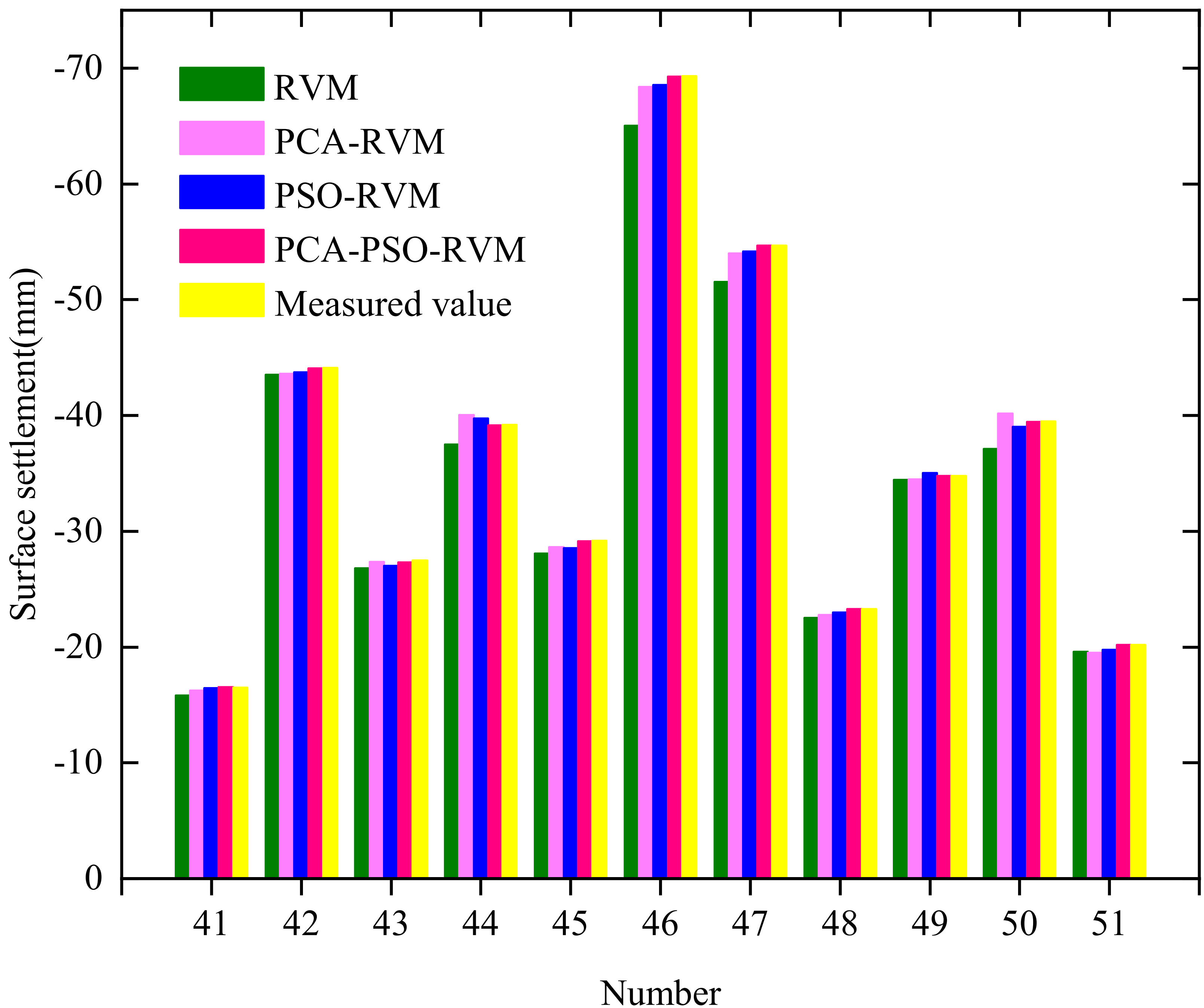

Figure

Click here to access/download;Figure;Fig. 7. (a) MRE.eps

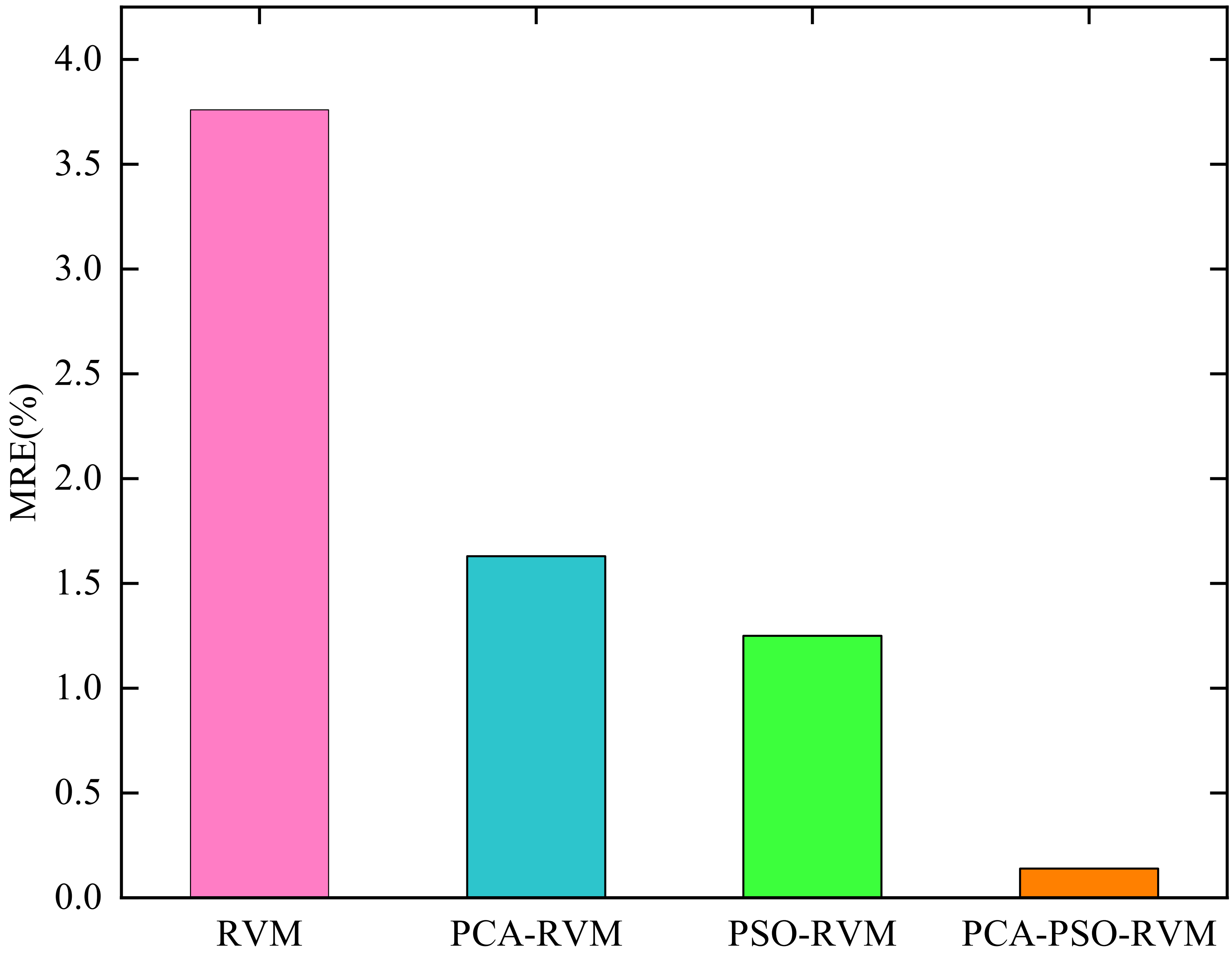

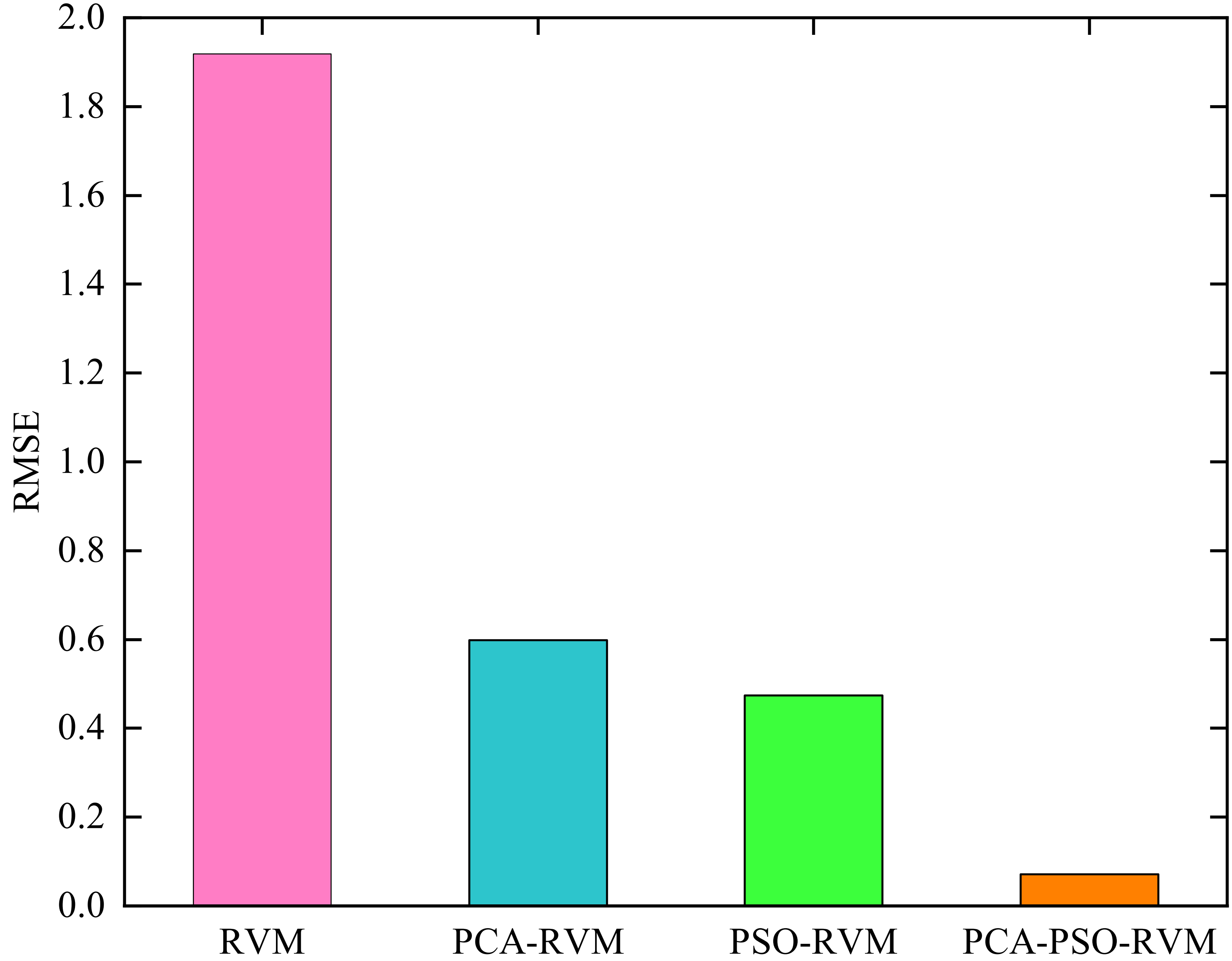
2.0
1.8
1.6
1.4
1.2
1.0
0.8
0.6
0.4
0.2
0.0
RMSE
RVM
PCA-RVM
PSO-RVM
PCA-PSO-RVM

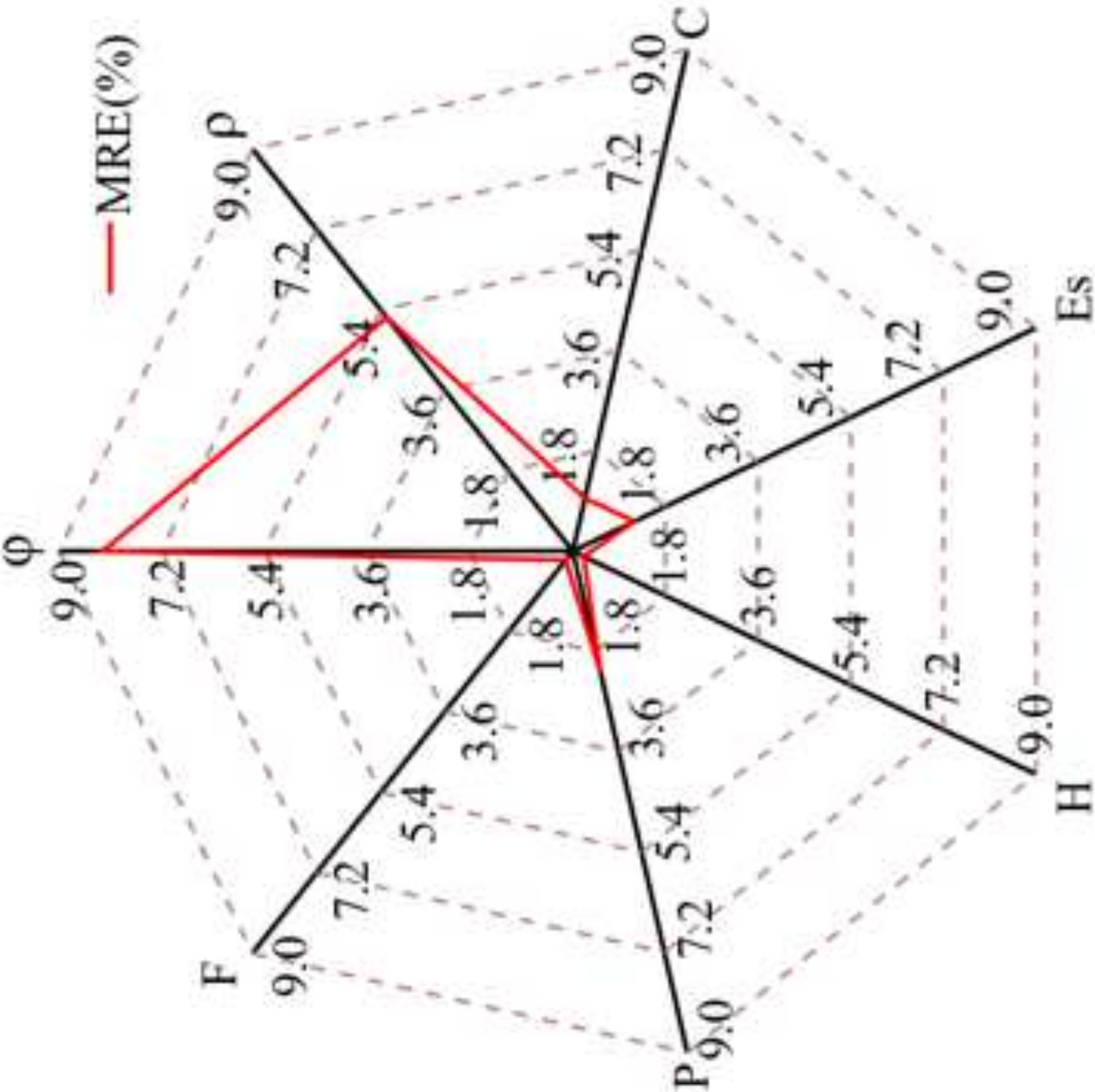
MRE(%)
φ
ρ
C
Es
H
P
F
1.8
3.6
5.4
7.2
9.0

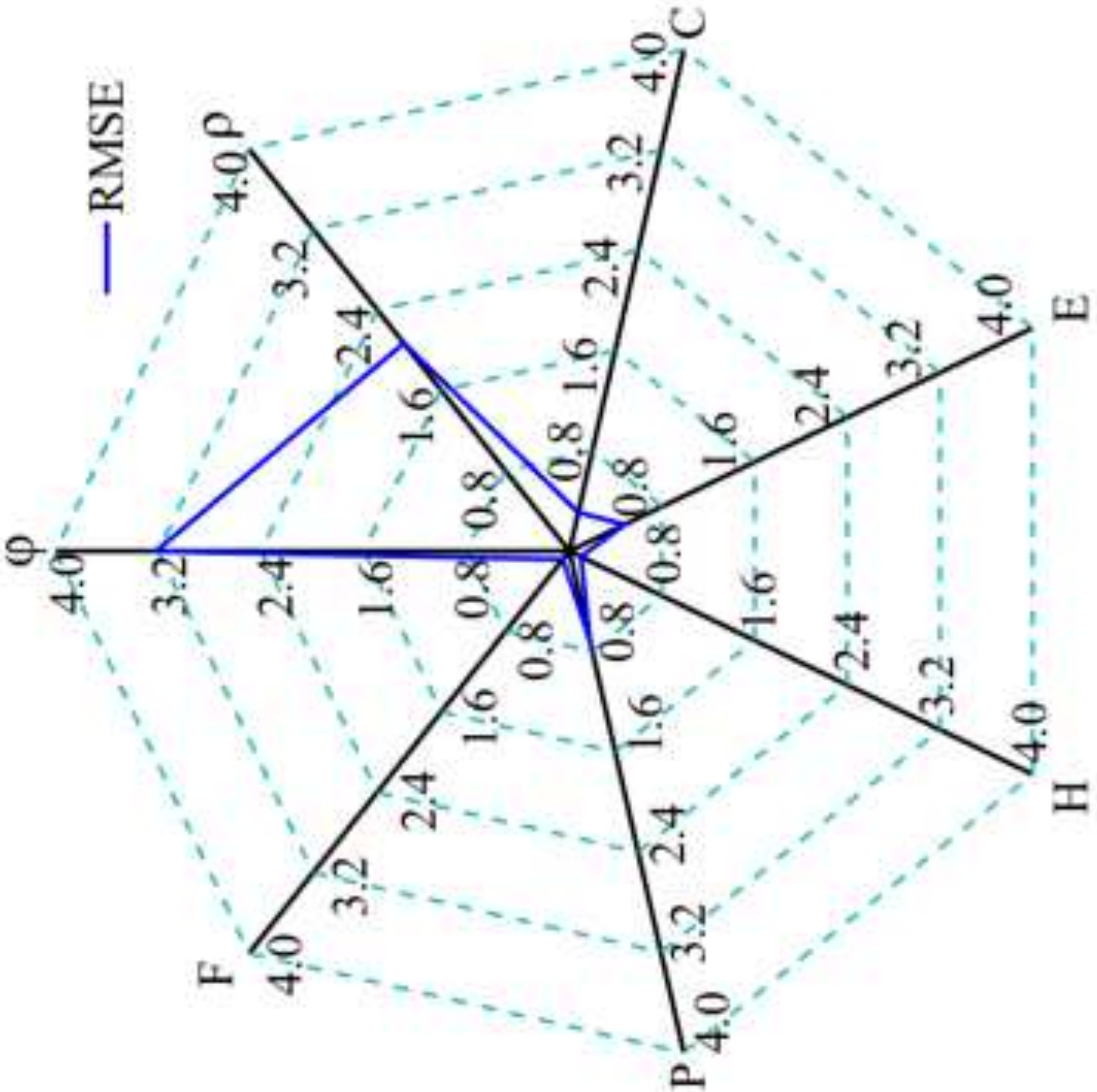
RMSE
φ
ρ
C
E
H
P
F
0.8
1.6
2.4
3.2
4.0

Figure

Click here to access/download;Figure;Fig. 8. Sensitivity factor analysis (c) TIC.eps

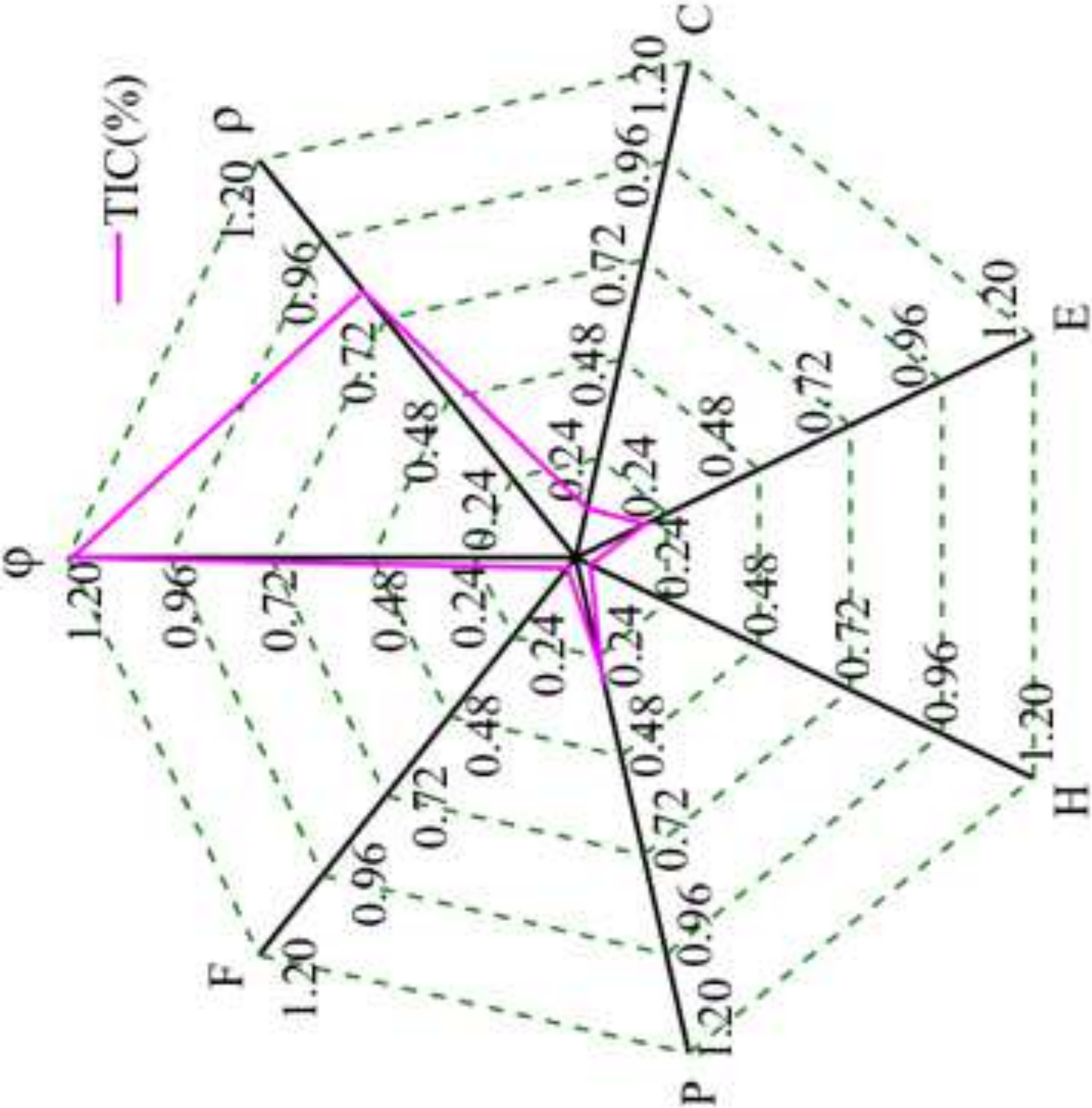

Figure Captions

Fig. 1. Schematic diagram of PCA

Fig. 2. Schematic diagram of RVM algorithm

Fig. 3. A schematic of PSO for solving the global optimization problem

Fig. 4. PCA results and analysis process: (a) PCA results; (b) Contribution rate of each factor and cumulative contribution rate.

Fig. 5. PCA-PSO-RVM model flow diagram

Fig. 6. Different methods for predicting results

Fig. 7. Comparison of MRE, RMSE and TIC in different methods: (a) MRE; (b) RMSE; (c) TIC.

Fig. 8. Sensitivity factor analysis: (a) MRE; (b) RMSE; (c) TIC.